

# Transmission System Geomagnetically Induced Current Model Validation

Maryam Kazerooni, *Student Member, IEEE*, Hao Zhu, *Member, IEEE*, Thomas J. Overbye, *Fellow, IEEE*, and David A. Wojtczak, *Member, IEEE*

**Abstract**—Geomagnetically induced currents (GICs) have the potential to severely disrupt power system operations by causing increased reactive power losses in the high-voltage transmission grid. This paper focuses on validating the model which relates the GICs to their deriving electric field. A novel validation framework is proposed with the advantage of considering the system uncertainties and network information availability. The effectiveness of this approaches is validated using both a 20 bus test system as well as actual GIC data provided by American Transmission Company.

**Index Terms**—Geomagnetic disturbance (GMD), geomagnetically induced currents (GICs), model validation, transmission system analysis.

## I. INTRODUCTION

SOLAR coronal holes and coronal mass ejections can disturb the Earth's geomagnetic field. These geomagnetic disturbances (GMD) in turn induce electric fields which drive low frequency currents in the transmission lines. These geomagnetically induced currents (GICs) can cause transformers half-cycle saturation which results in increased reactive power losses and harmonic currents. This may cause voltage instability by a combination of two means. First, the increased transformer reactive power losses might contribute directly to voltage instability. Second, the harmonic currents may cause relays malfunction and unintentional detachment of the reactive power resources such as static VAR compensators [1], [2].

Using actual data, when available, to validate the associated models helps to better understand the impacts of GICs on the power grid. GIC modeling has been widely studied [3]–[7]. It has been demonstrated that the transformer GIC relates to the electric field through a linear model, where the linear coefficients depend on the given power system parameters. A variety of commercial GIC flow solvers and a benchmark test case have also been developed [8].

Manuscript received February 11, 2016; revised June 14, 2016; accepted July 23, 2016. Date of publication August 1, 2016; date of current version April 17, 2017. This work was supported in part by the National Science Foundation through “Hazards SEES: Improved prediction of geomagnetic disturbances, geomagnetically induced currents, and their impacts on power distribution systems” and in part by the Illinois Center for a Smarter Electric Grid (ICSEG). Paper no. TPWRS-00230-2016.

M. Kazerooni, H. Zhu, and T. J. Overbye are with the Department of Electrical and Computer Engineering, University of Illinois, Urbana, IL 61801 USA (e-mail: kazerom2@illinois.edu; haozhu@illinois.edu; overbye@illinois.edu).

D. A. Wojtczak is with the American Transmission Company, Waukesha, WI 53188 USA (e-mail: dwojtczak@atcllc.com).

Color versions of one or more of the figures in this paper are available online at <http://ieeexplore.ieee.org>.

Digital Object Identifier 10.1109/TPWRS.2016.2596744

A key task in model validation is to reconstruct the system model during an event. For a geomagnetic storm, this includes using the magnetic field measurements to reproduce the electric field and the GICs. Reference [9] recreates the March 1989 storm for the Ontario high voltage network and validates the records of the GIC measurements accordingly. Various methods for modeling the neighboring networks during GMDs is presented in [10] and their effectiveness are validated for the Ontario-Montreal Network. This paper builds on the existing literature on the GIC model validation with more focus on the transmission-level study and also system uncertainty considerations. The goal is to identify the key challenges in model validation and eventually develop a general approach which addresses these issues.

There are at least three issues that need to be considered for GIC model validation. First, the exact information on the power system topology and dc conductance is hard to obtain, thus so are the linear coefficients. The substation grounding resistance is especially a key element in GIC modeling which is seldom available [11]. Second, the electric field needs to be estimated from the magnetic data and this estimation is not exact. Various methods have been developed to effectively determine the E-field through the magnetic and Earth conductivity data [12], yet this data is not accurate which introduces error to the resulting E-field. Last, the measured data mostly suffer from random noise and system perturbations. Hence, all the model components which include the linear coefficients, the input electric field, and measurement noise model are either unavailable or inaccurate. This emphasizes the need for validation techniques which are robust to such system uncertainties.

Singular value decomposition (SVD) is proposed in [13] to validate the GIC model using only the measurements and independent of the network information. SVD-based analysis successfully handles the system uncertainties and offers affective validation tools. However, it is desired to develop a technique with the ability to utilize the network parameters when they are available. Sometimes the network parameters are partially available with some degree of accuracy; and it is desired to take advantage of this additional information. This paper proposes a validation technique which improves over the SVD method by utilizing the available parameters. In this technique, the conventional GIC model is modified to account for the system uncertainties. Then, a validation framework is built upon this modified model. This framework is demonstrated using a small case study and its performance is evaluated. The effectiveness of the proposed technique in handling real system

uncertainties is validated through actual GIC data provided by American Transmission Company (ATC).

The paper is organized as follows: The GIC model is introduced in Section II. Model validation under system uncertainties is presented in Section III. Section IV demonstrates the proposed technique using the 20-bus test case, while the more interesting real data validation is given in Section V with transformer neutral current measurements from ATC. Section VI presents a conclusion and direction for future work.

## II. GIC MODELING

To calculate the voltage potential induced on the transmission line, the E-field is integrated over the length of the line. Assuming uniform E-field, the DC voltage on the line between bus  $n$  and  $m$  is expressed in:

$$V_{nm} = E^N L_{nm}^N + E^E L_{nm}^E \quad (1)$$

where  $L_{nm}^N$  and  $L_{nm}^E$  denote the northward and eastward line distances; and  $E^N$  and  $E^E$  are the northward and eastward E-fields, respectively. The induced voltages are converted to the dc current injections through Norton Equivalent, and the total current injections are derived from Kirchhoffs current law (KCL) [3]. The vector of current injections is obtained by putting all the current injections together as given by  $\mathbf{I}^{No} = \mathbf{C}\mathbf{E}$  where  $\mathbf{C}$  depends on the length, orientation and resistance of the lines.

The nodal network equations are written using KCL and the bus voltages are obtained from the current injections as expressed in:

$$\mathbf{V} = \mathbf{G}^{-1} \mathbf{I}^{No} \quad (2)$$

where matrix  $\mathbf{G}$  is similar to the bus admittance matrix except that it only captures the conductance values and is modified to include substation grounding resistances. The GICs are related to the bus voltages by Ohm's law:

$$\mathbf{I} = \mathbf{G}^S \mathbf{V} = (\mathbf{G}^S \mathbf{G}^{-1}) \mathbf{I}^{No} = (\mathbf{G}^S \mathbf{G}^{-1} \mathbf{C}) \mathbf{E} = \mathbf{H} \mathbf{E} \quad (3)$$

where  $\mathbf{G}^S$  is a diagonal matrix with the grounding resistances on its diagonal and  $\mathbf{H}$  is the coefficient matrix defined as  $\mathbf{H} := \mathbf{G}^S \mathbf{G}^{-1} \mathbf{C}$ . This linear model indicates that the GICs relate to the E-field through some constant coefficients. Matrix  $\mathbf{H}$  depends only on the network resistances and topology.

The GIC model represents the whole network and the vector  $\mathbf{I}$  includes the GICs at all transformers. Sometimes the whole network is not of interest, and it is desired to reduce the model to cover only specific transformers. To reduce the model, the entries of the  $\mathbf{I}$  vector corresponding to the specified transformers are selected and the coefficient matrix is truncated accordingly.

### A. Determination of the Transformers Coefficients

There are two coefficients associated with each transformer and the GIC model in (3) can be rewritten as:

$$\mathbf{I} = [\mathbf{H}^E \mid \mathbf{H}^N] \times \begin{bmatrix} E^E \\ E^N \end{bmatrix} \quad (4)$$

where  $H^E$  and  $H^N$  are the eastward and northward coefficients. An interesting observation is that the GICs are equal to the eastward coefficients when  $E^E$  is one and  $E^N$  is zero. Similarly, the GICs are equal to the northward coefficients when  $E^E$  is zero and  $E^N$  is one. This will be a basis for finding the coefficients as described in the following algorithm.

*Step 1:* An eastward E-field with unity magnitude is enforced to the system and the resulting GICs are calculated. According to (4), the eastward coefficients are equal to the GICs under this condition.

*Step 2:* A northward E-field with unity magnitude is enforced to the system and the northward coefficients are calculated similar to Step 1.

This algorithm requires calculation of the GICs induced by an enforced E-field. This can be done through basic circuit laws e.g. KVL, KCL and Ohms law. Alternatively, a commercial Power System Software may be used to conduct such calculations.

### B. Electric Field Estimation

The E-field is dynamic over the discrete time horizon  $\mathcal{T} := \{t^1, t^2, \dots, t^T\}$ , which can be concatenated into the  $2 \times T$  matrix:

$$\mathbf{X} = \begin{bmatrix} e^{E,t^1} & e^{E,t^2} & \dots & e^{E,t^T} \\ e^{N,t^1} & e^{N,t^2} & \dots & e^{N,t^T} \end{bmatrix} \quad (5)$$

where  $e^{N,t^n}$  and  $e^{E,t^n}$  are respectively the northward and eastward E-fields at the  $n$ th time instant. Similarly, the dynamic GIC vector  $\mathbf{I}$  forms the matrix:

$$\mathbf{Y} = \begin{bmatrix} z_1^{t^1} & z_1^{t^2} & \dots & z_1^{t^T} \\ z_2^{t^1} & z_2^{t^2} & \dots & z_2^{t^T} \\ \vdots & \vdots & \ddots & \vdots \\ z_K^{t^1} & z_K^{t^2} & \dots & z_K^{t^T} \end{bmatrix} \quad (6)$$

where  $z_k^{t^n}$  is the GIC reading of the  $k$ th sensor at the  $n$ th time instant and  $K$  is the total number of sensors. The GIC sensor is installed at the transformer neutral and measures the DC current passing through its neutral. The matrix form of the GIC model is expressed in:

$$\mathbf{Y} = \mathbf{H}\mathbf{X} + \mathbf{N} \quad (7)$$

where  $\mathbf{N}$  is the measurement noise. With the coefficient matrix available, the E-field is estimated from the GIC measurements using least squares estimation as given by [14]:

$$\hat{\mathbf{X}}^{LS} := \arg \min_{\mathbf{X}} \|\mathbf{Y} - \mathbf{H}\mathbf{X}\|_2 = (\mathbf{H}^T \mathbf{H})^{-1} \mathbf{H}^T \mathbf{Y} \quad (8)$$

where  $\hat{\mathbf{X}}$  is the estimated E-field and is assumed to be uniform within the footprint of the investigated transformers. This estimation is eventually compared with the one obtained from the magnetic field data to validate the model as illustrated in Fig. 1.

## III. MODEL VALIDATION UNDER ACTUAL MEASUREMENTS

In practice, the GIC model in (7) fails to represent the actual measurements as they are subjected to different types of noise

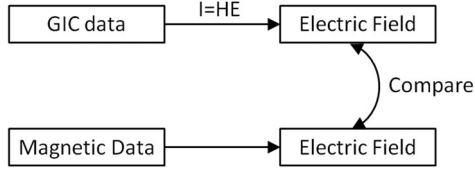


Fig. 1. GIC model validation framework based on GICs and magnetic measurements.

and system uncertainties. To account for such uncertainties, the GIC model is modified by introducing a scale for each measurement as given by:

$$\mathbf{Y} = \mathbf{S} \mathbf{H} \mathbf{X} + \mathbf{N} \quad (9)$$

where  $\mathbf{S}$  is a diagonal matrix with the scales on its diagonal. If properly defined, the scales can capture the system uncertainties. The GIC real data may be used to find such scales as described in the following algorithm.

---

**Algorithm 1:** Scales Calculation.

---

```

1: procedure SCALES CALCULATION ( $\mathbf{Y}, \mathbf{H}$ )
2:   Initialize all the priori scales to one:  $\mathbf{S} = \text{Diag}(\vec{1})$ .
3:   Initialize the posteriori scales to zero:  $\mathbf{S}^+ = \text{Diag}(\vec{0})$ .
4:   Define the convergence tolerance,  $\epsilon$ .
5:   while  $|\mathbf{S}^+ - \mathbf{S}| > \epsilon$  do
6:     Update the priori scales by  $\mathbf{S} = \mathbf{S}^+$ 
7:     Estimate the E-field using:
8:        $\hat{\mathbf{X}} = (\mathbf{H}^T \mathbf{S}^T \mathbf{S} \mathbf{H})^{-1} \mathbf{H}^T \mathbf{S}^T \mathbf{Y}$ .
9:     Calculate the posteriori scales by:
10:       $\mathbf{S}^+ = \text{Diag}(\mathbf{Y}) \text{Diag}^{-1}(\mathbf{H} \hat{\mathbf{X}})$ .
11:     Normalize the scales by  $\mathbf{S}^+ = \frac{K \mathbf{S}^+}{\text{Sum}(\mathbf{S}^+)}$ .
12:   end while
13:   return  $\mathbf{S}$ 
14: end procedure

```

---

In the algorithm,  $\text{Diag}()$  of a vector is a diagonal matrix with the vectors entries on its diagonal,  $\vec{1}$  is an all-one vector,  $\text{Sum}()$  of a matrix returns the sum of all its entries and  $K$  is the number of measurements.

The coefficient matrix depends on the network topology and resistances and its accuracy depends on the available network information. Most of the network parameters required for constructing the coefficient matrix are part of the standard power flow models and are accurately available. The only piece of information which may not be available, but has high impacts is the substation grounding resistance. Substation grounding resistance is the effective grounding resistance of the substation which includes the ground grid and the emanating ground paths due to shield wire grounding. Techniques are available in the literature to measure this parameter [17], yet many factors can compromise the measurement and consequently introduce error to the GIC model validation. First, external objects such as water pipelines and adjacent railroad tracks distort the earth potential contours. Second, sources of dc current such as dc railroad tracks, pipelines cathodic protection systems and dc transmission lines produce stray currents which interfere with the

grounding resistance measurements. Third, the resistance of the electrodes used for the measurements can introduce error if the substation being tested has low resistivity. Last, the grounding resistance mostly depends on the humidity, salt level or temperature and therefore is time-variant. Accurate measurement of the grounding resistance is very challenging and the available data (if any) is often inaccurate. Assigning the proper scales to the substation accounts for the inaccuracy of its grounding resistance.

The scales can be used to evaluate how well the GICs at a particular transformer agree with the model. In practice, not all the measurements conform to the model and some of the readings may exhibit different behavior. A possible reason for such divergent behaviors is non-uniform E-field. The linear GIC model is valid only when the E-field is uniform over the investigated area. When the geographic location of a transformer is too far from the others, its E-field may differ and its GIC will not agree with the model. The proposed scale estimation technique detect the outlier measurements by assigning them zero scale and eventually exclude them from the dataset. An example of using the scales to detect outliers will be provided later on.

Compared to the SVD-based analysis presented in [13], the proposed framework has several advantages owing to the additional network parameters. First, the proposed framework can validate the measurements independently and identify the ones which do not conform to the model whereas the SVD analysis determines the validity of the measurements all together without providing any insight on the individual measurements. Second, the proposed method provides additional tools for validating the parameters accuracy. The method utilizes the network parameters to estimate the E-field. Hence, the agreement between this estimation and the one from the magnetic field data validates the accuracy of the assumed parameters. Last, the proposed model provides more accurate E-field estimation compared to the SVD-based one which makes the validation framework built upon it more effective. Numerical results indicate that the first left singular of the SVD analysis perfectly captures the eastward E-field, yet the second left singular fails to estimate the northward E-field accurately. The comparison between the two methods will be provided later on through case studies as well as real data analysis and the advantages of the proposed technique discussed here will be demonstrated.

#### IV. NUMERICAL RESULTS USING A TEST CASE

In this section and the next, the effectiveness of the proposed validation technique is evaluated. This section uses the fictitious 20-bus system from [8] with the one-line diagram shown in Fig. 2, whereas in Section V the technique is evaluated using actual data GIC neutral currents for five transformers located in the ATC footprint for a GMD that occurred on March 9th, 2012. For consistency, the same March 9th, 2012 data will be used with the 20-bus case.

On March 9th the geomagnetic storm began at 2:00 UTC and reached a very high level in the following hours. The magnetic field data used here are from values measured at the US Geological Survey Fredericksburg Geomagnetic Observatory, located

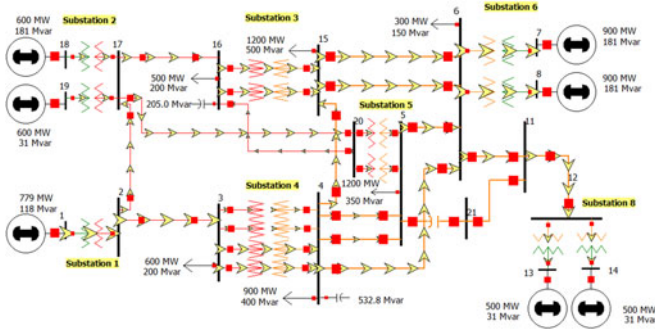


Fig. 2. Single-line diagram of the 20-bus test case in [8].

in the US at a latitude/longitude of  $38.205^\circ N$ ,  $77.373^\circ W$ . The reason for choosing this observatory is again, to maintain consistency with the results in Section V. The transformers used in Section V are located in the ATC footprint and Fredericksburg is the closest observatory to these transformers.

The E-field obtained from the Fredericksburg magnetic field is enforced on the system and the induced GICs are determined by solving the GIC flows using PowerWorld Simulator with the GIC add-on. White Gaussian random noise with signal-noise-ratio equal to 20 dB is added to the ideal GICs to simulate the system noise, and the synthetic measurements are obtained.

To evaluate the performance of the model validation framework under different uncertainties, three scenarios are considered each focusing on one type of uncertainty:

- 1) **Inaccurate Coefficients Scenario:** In this scenario, the available coefficients at the eighth and ninth transformers are two times larger than the actual ones (100% error). This could be caused by the inaccurate substation grounding resistances. In practice, the coefficients may have much lower error and this study considers the worst case scenarios.
- 2) **Outliers Scenario:** In this scenario, the measurements at the eighth and ninth transformers are enforced to be outliers. Outliers are considered to be measurements which are generated by a different E-field. The E-field data at The Natural Resources Canada Ottawa Geomagnetic Observatory is used to simulate the outliers whereas the normal measurements are generated by the Fredericksburg data. Ottawa observatory is located in Canada at a latitude/longitude of  $45.403^\circ N$ ,  $75.552^\circ W$ .
- 3) **Low Uncertainty Scenario:** This scenario considers the ideal case when the substation grounding resistances are accurate and no outlier exists in the measurements.

The transformer scales can account for the inaccurate coefficients. Fig. 3 illustrates the scales under the first scenario where the assumed coefficients at the eighth and ninth transformers are double the actual ones. According to the figure, the scales for these transformers take the value of 0.5 to compensate for this inaccuracy. A correct estimate of the coefficients can be obtained through multiplying the assumed coefficients by their corresponding scales as shown in Fig. 4.

The transformer scales can be used to detect the measurement outliers as illustrated in Fig. 5. The readings from the eighth and

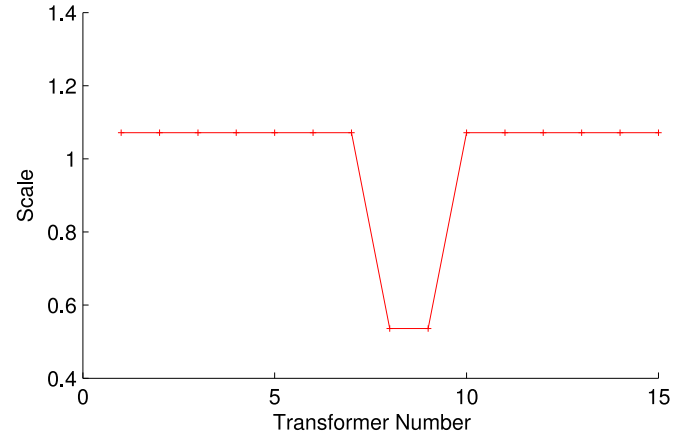


Fig. 3. The transformer scales under the inaccurate coefficients scenario.

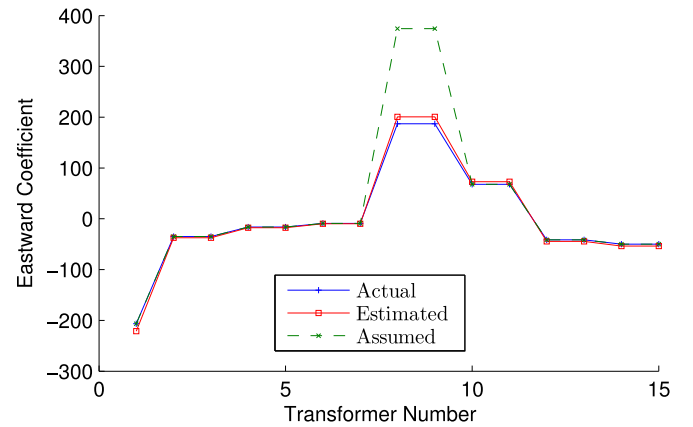


Fig. 4. Correcting the inaccurate coefficients through the scales.

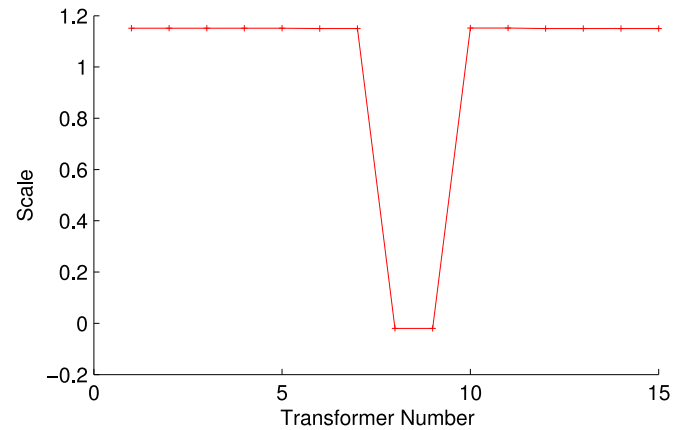


Fig. 5. The transformer scales under the outlier scenario.

ninth transformers are enforced to be outliers and the scale estimation technique successfully detects them and eliminates them from the model by assigning them zero scales.

The 20-bus system has two shunt capacitors at bus 4 and 16. Numerical results indicate that disconnecting these capacitors does not affect the proposed framework. This is because the



TABLE I  
ACCURACY COMPARISON OF THE E-FIELD ESTIMATION TECHNIQUES  
FOR THE TEST CASE

Estimation Technique	Eastward E-Field			Northward E-Field		
	Scen1	Scen2	Scen3	Scen1	Scen2	Scen3
Proposed	1.000	1.000	1.000	1.000	1.000	1.000
Conventional	0.997	0.992	1.000	0.999	0.998	1.000
SVD	0.974	0.927	0.974	0.710	0.591	0.710

GIC calculation is based on steady state dc analysis in which the capacitors act as open circuit. Hence, disconnecting them does not change the GIC model. The effect becomes significant when AC analysis is performed as opposed to dc. Power flow is solved including GICs and it is observed that connecting the shunt capacitors provides reactive power support and improves the voltage profile. The framework is robust to power filters and static synchronous compensator devices as well since they only affect the AC analysis and not the dc.

Next, the performance of the proposed model is compared with the SVD-base technique presented in [13]. Table I presents the accuracy of the two methods in estimating the E-field. For reference, the results for the conventional model in (7) is also included. Pearson correlation coefficient is used to measure the correlation between the estimated and the actual E-field with the following definition:

$$\rho_{X,Y} = \frac{\text{cov}(X,Y)}{\sigma_X \sigma_Y} \quad (10)$$

where  $\rho_{X,Y}$  and  $\text{cov}(X,Y)$  are the Pearson correlation and covariance between signals  $X$  and  $Y$ , respectively, and  $\sigma$  is the standard deviation. The comparison is performed for the three uncertainty scenarios described earlier which are “Inaccurate Coefficients”, “Outliers”, and “Low Uncertainty”. These scenarios are denoted by “Scen1”, “Scen2” and “Scen3” in the table, respectively. In the east direction, all three methods estimate the E-field accurately under all three uncertainty scenarios and their corresponding correlation coefficients are always larger than 0.92. For the northward E-field, the proposed model and the conventional one provide accurate estimation, whereas the estimate from the SVD-based technique is not accurate with its correlation coefficient reaching as low as 0.59.

Fig. 6 illustrates the actual E-field in east direction as compared with the estimates obtained from the proposed model and the SVD analysis. The fields are scaled to have unit Euclidean norm. The agreement between the estimated and actual fields verifies the accuracy for both methods. Fig. 7 demonstrates similar comparison for E-field in north direction. In this direction, the estimate from the proposed model has extremely high agreement with the actual field whereas the SVD analysis fails to provide good accuracy. The estimate from the conventional model is not included in Fig. 6 and Fig. 7 for better clarity, as it is perfectly aligned with the estimate from the proposed model. The E-field estimated by the conventional model differs from the one from the proposed model only by a scaling factor and hence, the normalized fields in the figures are aligned.

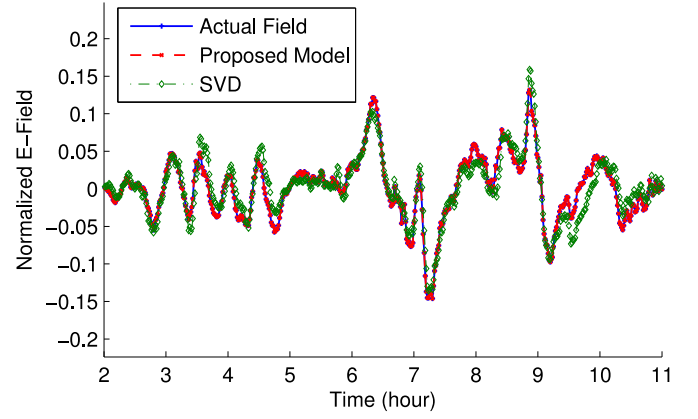


Fig. 6. Comparison of the eastward E-field estimation using different methods for the test case.

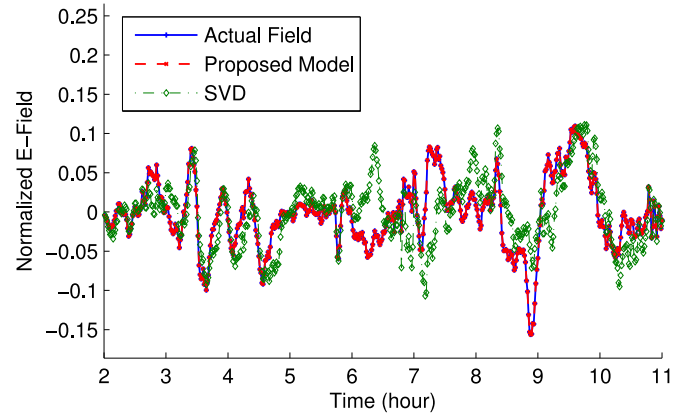


Fig. 7. Comparison of the northward E-field estimation using different methods for the test case.

TABLE II  
PERCENTAGE ERROR NORM IN ESTIMATING GICs BASED  
ON DIFFERENT TECHNIQUES

Estimation Technique	Scen1	Scen2	Scen3
Proposed	4.91%	5.22%	5.01%
Conventional	48.29%	66.45%	5.01%
SVD	4.91%	5.21 %	5.00%

The last validation test is to study the accuracy of different techniques in estimating the individual GIC measurements. The E-field estimated by the conventional and proposed model are used in their corresponding GIC flow equations which are (7) for the conventional model and (9) for the proposed one; and the estimated GICs are obtained. This estimation is then compared with the actual GICs which was initially used to estimate the E-field. SVD-base technique estimates GICs through rank-two approximation. Table II presents the estimation error for the investigated techniques with error defined as

$$\text{Error} = \frac{\|\hat{\mathbf{Y}} - \mathbf{Y}\|_F}{\|\mathbf{Y}\|_F} \quad (11)$$

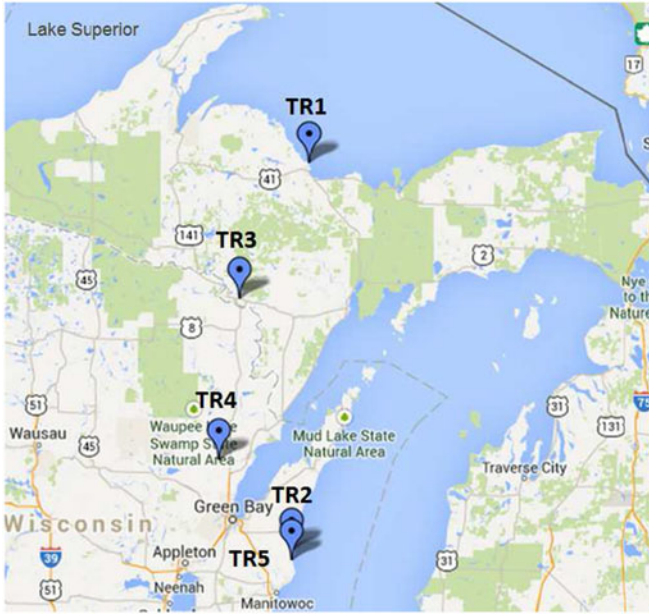


Fig. 8. Geographic location of the investigated ATC transformers.

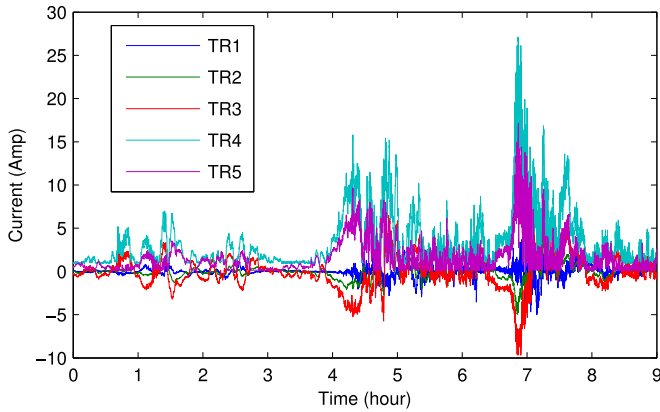


Fig. 9. GICs at investigated ATC transformers on March 9th, 2012.

where  $\hat{\mathbf{Y}}$  is the matrix of estimated GICs and  $\|\cdot\|_F$  is the Frobenius norm. It is observed that the SVD analysis and the proposed model estimate the GICs accurately for under all uncertainty scenarios. The conventional model estimates the GICs accurately under the ideal scenario, but its estimation error increases up to 66% in the presence of grounding resistance uncertainty or outliers.

## V. NUMERICAL RESULTS FOR REAL DATA

In this section, the GIC model is validated using real data measurements provided by ATC. This study focuses on the neutral current measurements of five transformers near the Wisconsin/Michigan area with the locations illustrated in Fig. 8. The geographical proximity of the Fredericksburg magnetometer to the ATC footprint makes using its data relevant to this study.

The GIC data for the March 9th, 2012 storm is chosen primarily for the analysis, as plotted in Fig. 9. The transformers

are indexed from 1 to 5. The highest GIC observed at these transformers is 27 A. Records of previous storms indicate that GICs can reach up to 330 A for more vulnerable locations and more severe storms [2]. Such observations indicate that the existing infrastructure including the shielding techniques does not protect the substations from GMDs. The GICs are derived from the E-field induced over long transmission lines and are sank into the ground through the substation grounding. The shielding techniques may protect a small range, but fail to block the GICs coming from long transmission lines. It is observed that at the transformers TR4, and TR5, the absolute value of the current is measured and the direction is missing. An effective data preprocessing technique is used to retrieve the direction as presented in the following.

### A. Data Preprocessing

The set of GIC measurements may be divided in to two groups: 1) the measurements that have the direction information (directed GICs) and 2) the measurements which are missing direction (undirected GICs). The matrix containing the GICs may be rearranged to separate the directed measurements from the undirected ones as expressed in:

$$\mathbf{Y} = \begin{bmatrix} \mathbf{Y}_D \\ \mathbf{Y}_U \end{bmatrix}, \mathbf{H} = \begin{bmatrix} \mathbf{H}_D \\ \mathbf{H}_U \end{bmatrix} \quad (12)$$

where  $\mathbf{Y}_D$  and  $\mathbf{Y}_U$  are the matrices of the directed and undirected GICs, respectively, and  $\mathbf{H}_D$  and  $\mathbf{H}_U$  are their corresponding coefficient matrices. The electric field can be estimated from the directed GICs using least squares estimation:

$$\hat{\mathbf{E}}^{LS} = (\mathbf{H}_D^T \mathbf{H}_D)^{-1} \mathbf{H}_D^T \mathbf{Y}_D. \quad (13)$$

Once the E-field is determined, an initial estimate of the undirected GICs are obtained through:

$$\hat{\mathbf{Y}}_U^- = \mathbf{H}_U \hat{\mathbf{E}}^{LS} \quad (14)$$

Finally, the direction of this estimate is utilized to retrieve the direction of the actual measurement as given by

$$\hat{\mathbf{Y}}_U^+ = \text{sign}(\hat{\mathbf{Y}}_U^-) \cdot \mathbf{Y}_U \quad (15)$$

where  $\hat{\mathbf{Y}}_U^+$  is the final estimate of the undirected GICs, and  $\hat{\mathbf{Y}}_U^-$  is their initial estimate.

The proposed technique is applied to the measurements at “TR4” and “TR5”, and their directions are retrieved. The actual data at “TR4” and its preprocessed result is presented in Fig. 10. For reference, the GIC at “TR2” is presented as well. The preprocessed data has strong correlation with the data at “TR2” which validates the effectiveness of this technique.

### B. GIC Model validation

To perform the GIC model validation, first the transformers coefficients are calculated. The investigated transformers are part of the eastern interconnect (EI). The EI system is simulated in PowerWorld Simulator using the available network parameters and the coefficients are calculated based on the method

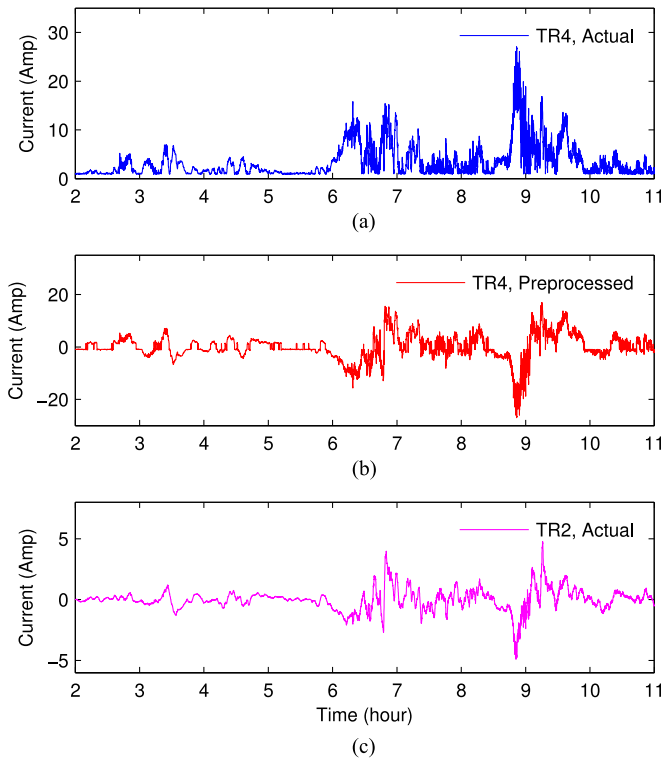


Fig. 10. Proposed data preprocessing Technique. (a) Actual and (b) preprocessed data for transformer “TR4”. (c) Actual data for the transformer “TR2”.

TABLE III  
GROUNDING RESISTANCE AND COEFFICIENTS OF INVESTIGATED  
ATC TRANSFORMERS

Name	$H^E$	$H^N$	$R_g$
TR1	20.816	25.831	0.168
TR2	21.5	34.4	0.222
TR3	-13.8	4.2	0.168
TR4	-14.875	18.818	0.181
TR5	3.2	2.14	0.148

described earlier. Unfortunately, the grounding resistances are not available for the EI system and a simplistic model was used to estimate their values. The assumed grounding resistances and the resulting coefficients are presented in Table III.

In theory, all parts of the network should be considered for calculating the coefficients. However, studies show that the GIC impacts are localized and considering only the nearby areas provides sufficient accuracy. In the current study, all the EI areas are included in the calculations, yet later investigations demonstrated that this was not necessary and considering only the areas near Wisconsin provided sufficient accuracy.

There are two GIC models to be validated: The conventional model in (7) and the modified one in (9) with the introduced scales. The model validation framework is used to evaluate the effectiveness of these models through real data analysis.

Fig. 11 illustrates how well each individual measurement agrees to the conventional model. First, the E-field is estimated from the GIC measurements through the conventional model

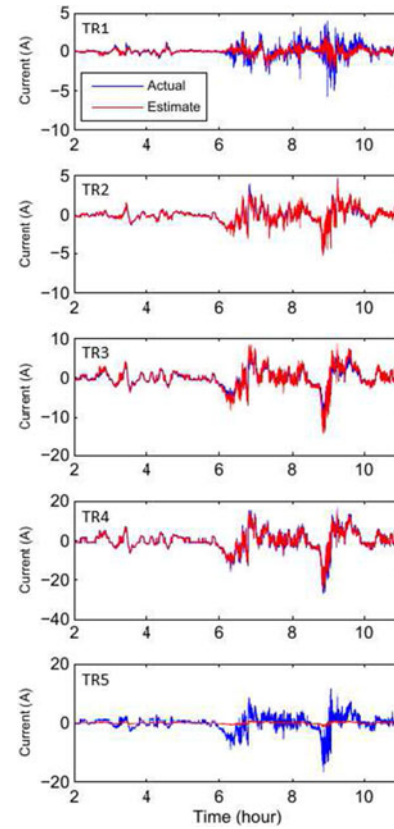


Fig. 11. Accuracy of the conventional model in estimating the GICs.

as proposed in (8). The estimated E-field is multiplied by the transformer coefficients to get the estimated GIC using  $\mathbf{I} = \mathbf{H}\mathbf{E}$ . This estimation is then compared with the actual measurement. According to the figure, the estimated and actual GICs have very good agreement at “TR2”, “TR3”, and “TR4”. The estimate at “TR1” does not agree well with the actual GIC, but still has the same order of magnitude. The worst agreement is at “TR5” where the estimate is almost zero, even though the actual GIC reaches up to 20 A. Going back to Table III, the coefficients for “TR5” are 3.2 and 2.14 in east and north direction, respectively. These values are very small compared to the other transformers, e.g., the coefficients of “TR1” are 20.8 and 25.8. “TR5” coefficients are expected to be larger since its measured GIC is in the same order as the other transformers. This casts doubt on the accuracy of the assumed coefficients. The modified model may be used to correct the inaccurate coefficients through the scales as will be demonstrated shortly.

The modified model accounts for the system uncertainties and in particular, the inaccurate coefficients. Fig. 12 compares the estimated GICs obtained from the modified model with the actual measurements. This time, the estimated GIC at “TR5” have high agreement with the actual one which confirms that the modified model account for the inaccurate coefficients by assigning a larger scale to “TR5”. Another interesting observation is that the estimated GIC at “TR1” is close to zero. This is because the modified model assigns a very small scale to “TR1” which reduces the estimated GIC to almost zero. Recall that the

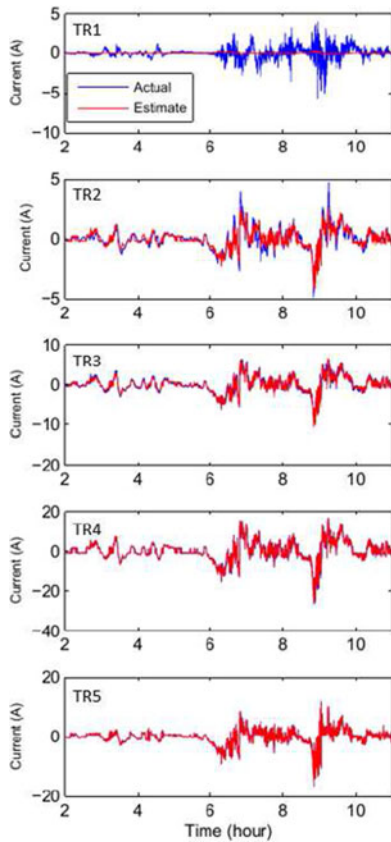


Fig. 12. Accuracy of the modified model in estimating the GICs.

TABLE IV  
PEARSON CORRELATION COEFFICIENTS BETWEEN THE GICs

Name	TR1	TR2	TR3	TR4	TR5
TR1	1	-0.166	0.072	0.117	0.051
TR2	-0.166	1	0.791	0.652	0.651
TR3	0.072	0.791	1	0.700	0.653
TR4	0.117	0.652	0.700	1	0.883
TR5	0.051	0.651	0.653	0.883	1

modified model assigns zero scales to the outlier measurements as was demonstrated through an example in previous section (see Fig. 5). Similar to the example case, the measurement at “TR1” has irregularity, and hence gets a zero scale. It is clear in Fig. 12 that all the measurements are correlated except for “TR1”. This can be confirmed using the Pearson correlation coefficients as presented in Table IV. The value at row “TR $X$ ” and column “TR $Y$ ” of the table is the coefficient between the GICs at transformers  $X$  and  $Y$ . Pairwise comparison of these coefficients confirms the weak correlation for “TR1”.

Many factors could contribute to zeroing out the scale of a transformer. One possible reason is having a different E-field than the rest of the network in which case, the uniform E-field assumption does not hold and the GIC model is not valid anymore. Hence, the transformer with a different E-field is excluded from the model by setting its scale to be zero. “TR1” is located in the northern part of Michigan and is on the shores of Lake Su-

TABLE V  
ACCURACY COMPARISON OF THE E-FIELD ESTIMATION TECHNIQUES FOR THE ATC SYSTEM

Estimation Technique	Eastward Field	Northward Field
Proposed	0.629	0.740
Conventional	0.656	0.737
SVD	0.630	0.016

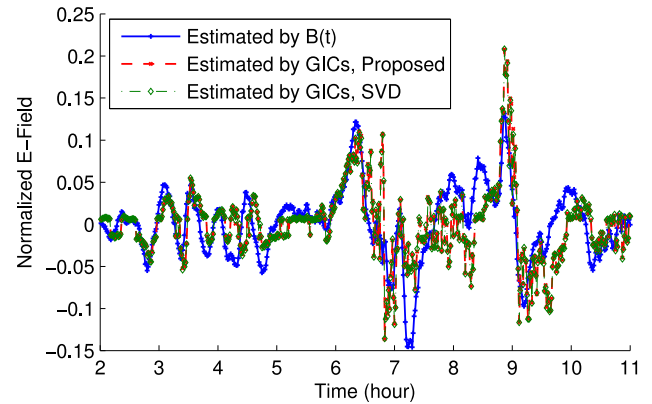


Fig. 13. Comparison of the eastward E-field estimation using different methods for the ATC system.

prior as shown in Fig. 8. Its higher latitude as well as the nearby body of water could result in a different E-field and eventually zeroing out the scale.

The ultraviolet emission measurements obtained from Special Sensor Ultraviolet Spectrograph Imager (a remote-sensing instrument mounted on a satellite) can provide auroral environmental data records (EDRs) with information on the electron energy flux ( $Q$ ), the magnetic field lines and the auroral boundaries during a solar storm [18]. Analysis of the auroral EDRs for the March 9, 2012 storm indicates that the aurora moved to the lower latitudes during the storm. The Aurora even hit the Ottawa magnetic observatory as confirmed with its magnetic field measurements. This suggests that the irregularity at “TR1” could be due to the magnetic disturbances associated with the aurora. Further exploration into the E-field at the transformer “TR1” and why its scale vanishes will be an interesting future study.

The performance of the proposed technique is compared with the SVD-based approach. The E-field estimated from the magnetic data is compared with the estimate from GIC measurements using both methods and their Pearson correlation coefficients are presented in Table V. For reference, the results for the conventional GIC model in (7) are also included in the table. All three methods estimate the Eastward E-field quite accurately with their correlation coefficients around 0.6. The proposed model and the conventional one estimate the Northward E-field with relatively good accuracy whereas the estimate from the SVD-based approach is extremely inaccurate with its correlation coefficient equal to 0.016.

Fig. 13 presents the eastward E-field obtained from the magnetic data as compared with the estimate from the GIC



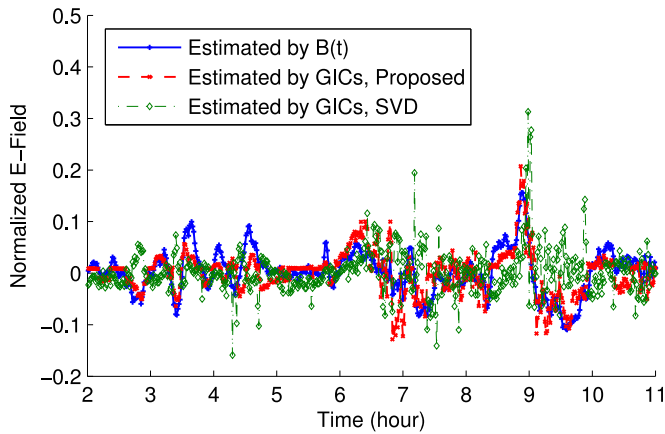


Fig. 14. Comparison of the northward E-field estimation using different methods for the ATC system.

measurements using both the proposed model and the SVD analysis. The fields are scaled to have unit Euclidean norm. The estimate from both methods has good agreement with the one from the magnetic data. Fig. 14 demonstrates similar comparison for the E-field in north direction. In this direction, the estimate from the proposed model has relatively good agreement with the one from the magnetic data whereas the estimate from SVD analysis has significant mismatches. For better clarity, the estimate from the conventional model is not included in Figs. 6 and 7 as it is perfectly aligned with the estimate from the proposed model.

## VI. CONCLUSION

In this paper, a novel validation technique is presented which utilizes the network parameters to provide stronger validation tools. This method introduces the transformer scales to account for the system uncertainties and provides the extra capability of detecting the outlier measurements. The proposed validation framework is demonstrated using a small case study and its performance is extensively studied under different scenarios. More interesting real data validation is conducted using the GIC measurements provided by ATC. The data from five transformers are validated, the inaccurate model parameters are adjusted through the scales and finally, the existing outlier in the set of the measurements is successfully detected.

The paper suggests several opportunities for future research. First, the technique presented here enables outlier detection, but does not provide any explanation for the existing abnormalities. Presently, one of the ATC transformers is discovered as outlier, but the question of why it has such divergent behavior stays unanswered. Future research tends to answer this question by looking at possible factors such as different E-field, the nearby body of water, or ground resistance. Second, the current validation framework can be used to estimate the unknown parameters such as the substation grounding resistance. Further enhancements to the parameter-based validation scheme are currently being pursued toward this goal.

## ACKNOWLEDGMENT

The authors are thankful for the data provided by the American Transmission Company (ATC).

## REFERENCES

- [1] V. D. Albertson, J. M. Thorson, R. E. Clayton, and S. C. Tripathy, "Solar-induced-currents in power systems: Cause and effects," *IEEE Trans. Power App. Syst.*, vol. PAS-92, no. 2, pp. 471–477, Mar. 1973.
- [2] North American Electric Reliability Corporation (NERC), "2012 special reliability assessment interim report: Effects of geomagnetic disturbances on the bulk power system," Tech. Rep., Feb. 2012.
- [3] D. H. Boteler and R. J. Pirjola, "Modeling geomagnetically induced currents produced by realistic and uniform electric fields," *IEEE Trans. Power Del.*, vol. 13, no. 4, pp. 1303–1308, Oct. 1998.
- [4] V. D. Albertson, J. G. Kappenman, N. Mohan, and G. A. Skarbakka, "Load-flow studies in the presence of geomagnetically-induced currents," *IEEE Trans. Power App. Syst.*, vol. PAS-100, no. 2, pp. 594–607, Feb. 1981.
- [5] J. Kappenman, "Geomagnetic Storms and Their Impacts on the U. S. Power Grid," Metatech Corp., Goleta, CA, USA, Tech. Rep. Meta-R-319, Jan. 2010.
- [6] R. A. Walling and A. N. Khan, "Characteristics of transformer exciting-current during geomagnetic disturbances," *IEEE Trans. Power Del.*, vol. 6, no. 4, pp. 1707–1714, Oct. 1991.
- [7] T. J. Overbye, T. R. Hutchins, K. Shetye, J. Weber, and S. Dahman, "Integration of geomagnetic disturbance modeling into the power flow: A methodology for large-scale system studies," in *Proc. North Amer. Power Symp.*, Sep. 2012, pp. 1–7.
- [8] R. Horton, D. H. Boteler, T. J. Overbye, R. J. Pirjola, and R. Dugan, "A test case for the calculation of geomagnetically induced currents," *IEEE Trans. Power Del.*, vol. 27, no. 4, pp. 2368–2373, Oct. 2012.
- [9] A. Yan, D. Zhou, and L. Marti, "Analysis of geomagnetically induced currents," in *Proc. IEEE Power & Energy Soc. General Meeting*, Jul. 2013.
- [10] D. H. Boteler, A. J. C. Lackey, L. Marti, and S. Shelemy, "Equivalent circuits for modelling geomagnetically induced currents from a neighbouring network," in *Proc. IEEE Power & Energy Soc. General Meeting*, Jul. 2013, pp. 1–5.
- [11] R. Pirjola, "Study of effects of changes of earthing resistances on geomagnetically induced currents in an electric power transmission system," *Radio Sci.*, vol. 43, 2008, Art. no. RS1004.
- [12] L. Marti, A. Rezaei-Zare, and D. Boteler, "Calculation of induced electric field during a geomagnetic storm using recursive convolution," *IEEE Trans. Power Del.*, vol. 29, no. 2, pp. 802–807, Apr. 2014.
- [13] M. Kazerooni, Z. Hao, and T. J. Overbye, "Singular value decomposition in geomagnetically induced current validation," in *Proc. IEEE Power & Energy Soc. Innovative Smart Grid Technol. Conf.*, Feb. 2015, pp. 1–5.
- [14] M. Kazerooni, Z. Hao, K. Shetye, and T. J. Overbye, "Estimation of geoelectric field for validating geomagnetic disturbance modeling," in *Proc. Power Energy Conf. Illinois*, Feb. 2013, pp. 218–224.
- [15] T. J. Overbye, K. S. Shetye, T. R. Hutchins, Q. Qiu, and J. D. Weber, "Power grid sensitivity analysis of geomagnetically induced currents," *IEEE Trans. Power Syst.*, vol. 28, no. 4, pp. 4821–4828, Nov. 2013.
- [16] International Real-time Magnetic Observatory Network. [Online]. Available: <http://www.intermagnet.org/>
- [17] *IEEE Guide for Measuring Earth Resistivity, Ground Impedance, and Earth Surface Potentials of a Grounding System*, IEEE Std. 81-2012 (Revision of IEEE Std. 81-1983).
- [18] Special Sensor Ultraviolet Spectrograph Imager. [Online]. Available: <http://ssusi.jhuapl.edu/>

**Maryam Kazerooni** (S'11) was born in Shiraz, Iran. She received the B.S. and M.S. degrees, both in electrical engineering, from Sharif University of Technology, Tehran, Iran, and the University of Windsor, Windsor, ON, Canada, in 2010 and 2012, respectively. She is currently working toward the Ph.D. degree in electrical engineering in the University of Illinois, Urbana-Champaign, Champaign, IL, USA.

Her current research interests include power system reliability, state estimation, and geomagnetic disturbance analysis.

**Hao Zhu** (M'12) received the B.S. degree from Tsinghua University, Beijing, China, in 2006, and the M.Sc. and Ph.D. degrees from the University of Minnesota, Minneapolis, MN, USA, in 2009 and 2012, respectively.

He is currently an Assistant Professor of electrical and computer engineering at University of Illinois, Urbana-Champaign. Her current research interests include power system monitoring and operations, dynamics and stability, and energy data analytics.

**Thomas J. Overbye** (S'87–M'92–SM'96–F'05) was born in Milwaukee, WI, USA. He received the B.S., M.S., and Ph.D. degrees in electrical engineering from the University of Wisconsin-Madison, Madison, WI, USA.

He is currently the Fox Family Professor of Electrical and Computer Engineering at the University of Illinois, Urbana-Champaign, Champaign, IL, USA. His current research interests include power system visualization, power system dynamics, power system cyber security, and power system geomagnetic disturbance analysis.

**David A. Wojtczak** (M'05) was born at Camp Gordon, GA, USA. He received the B.S. degree in electrical engineering from the University of Wisconsin, Milwaukee, WI, USA.

He began his career at Wisconsin Electric in September 1980, working in distribution planning, distribution development, and power plant engineering until 1989. He joined American Transmission Company (ATC) in January 2001, and is currently the Team Leader of Substation Services, ATC, Pewaukee, WI, USA. His current interests include membership on the NERC Geomagnetic Disturbance Task Force, substation design, physical security of substations, and research on GMD mitigation devices. He is a Member of Tau Beta Pi and is a registered Professional Engineer in Wisconsin.